ACOUSTICAL PROBING FOR MICROBUBBLES AT SEA

by

Herman Medwin
Department of Physics and Chemistry
Naval Postgraduate School
Monterey, California 93940
U.S.A.

ABSTRACT

Free gas bubbles have been indicted for many physical processes at sea including: scavenging detritus and chemicals from the ocean volume; generating droplets whose salts affect thunderstorm activity over the sea; providing cavitation nuclei; producing sound scatter and sound attenuation. It is the latter two phenomena that make acoustic measurements the most promising pathway for conducting a census of bubble populations. In particular, the very large scattering and extinction cross sections of a bubble at resonance, and the dispersion of sound speed in bubbly water, have made it possible to recently obtain marine bubble populations as a function of radius from 20 to 300 microns at depths to 15 metres. The growing knowledge of bubble numbers and behaviour will, in turn, permit more accurate predictions of sound propagation and fluctuations, particularly near the sea surface.

1. Review of Bubble Theory

1.1 Single Bubbles

Acousticians know very well that when a gas bubble in water senses a frequency at or near its natural frequency it will very effectively absorb and scatter that sound. At resonance, the scattering and absorption cross-sections of a typical bubble at sea are of the order 1000 times its geometrical cross-section and 10^8 times the scattering cross-section of a rigid sphere of the same radius. See Figure 1.1

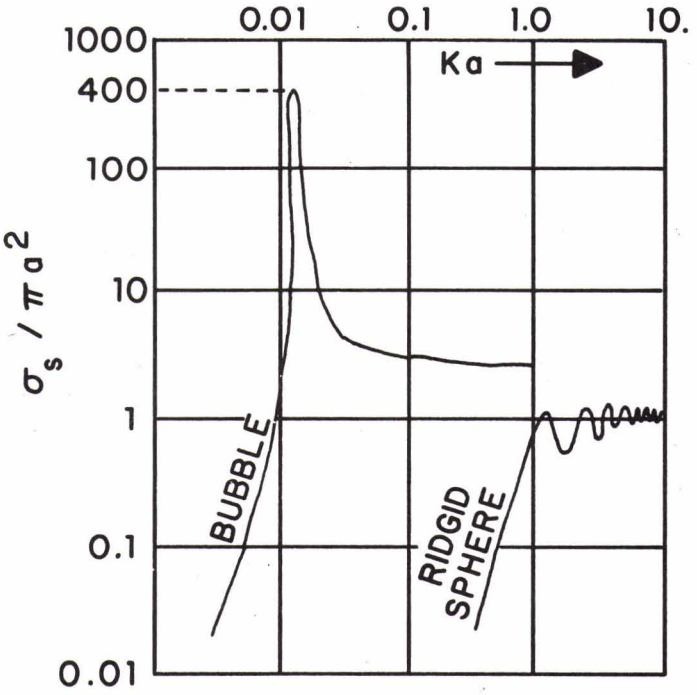

FIG. 1.1
RATIO OF SCATTERING CROSS SECTION, σ_s, TO GEOMETRICAL CROSS SECTION FOR BUBBLE AND RIGID SPHERE. k IS WAVE NUMBER IN WATER

Our first need is to review the behavior of single bubbles in order to determine the effect of the bubble parameters on the resonance frequency, damping constants and acoustical cross sections. We will then consider the propagation of sound in bubbly water.

To calculate the natural body frequency at which a bubble resonates, assume for simplicity that the motion of the bubble is completely accounted for by two factors: a) the compressibility of the enclosed gas during reversible expansion and compression with no heat exchange (adiabatic oscillation); and b) the liquid mass moved by the bubble as it oscillates. For the present we will assume that the damping is negligible and that there are no effects due to surface tension or thermal conductivity.

a) Bubble Stiffness: Start with the adiabatic gas relation, pV^{γ} = constant where p is the instantaneous total pressure within the bubble volume, V. The constant, γ, is the ratio of specific heats for the enclosed gas. Differentiating yields

$$\frac{P_i}{dV} = \frac{\gamma P_o}{V}$$

where P_i, the instantaneous incremental pressure is $p - P_o$; P_o is ambient pressure ($P_o >> |p_i|$); dV is incremental volume.

The stiffness restoring force acting over the entire spherical surface is

$$F_r = 4\pi a^2 p_i = - (12\pi\gamma P_o a)\xi \qquad (1.1.1)$$

Equation (1.1.1) is in the form of Hooke's Law where a is the average radius of the bubble. The quantity in parentheses is the stiffness constant, s_A; the subscript, A, refers to adiabatic and other assumptions.

$$s_A = 12\pi\gamma P_o a \qquad (1.1.2)$$

b) Bubble Mass: The major part of the oscillating mass is due to the liquid adjacent to the bubble rather than the mass of the gas. The inertial force acting over the bubble surface is determined by calculating the pressure of the reradiated sound. Later we will verify that, at resonance, $ka << 1$, where k is the wave number in water, and that the scattered pressure wave is therefore isotropic and is given by

$$\underset{\sim}{p_s} = \frac{\sqrt{2}\, P_{\dot{m}S}}{R} \exp\,[i(\omega t - kR)] \qquad (1.1.3)$$

where $\underset{\sim}{P}_s$ is the rms scattered pressure at 1 m radius.

The acoustic momentum equation in spherical coordinates has the radial component

$$\rho \ddot{\xi} = - \frac{\partial p_s}{\partial R}$$

where ρ is water density. At the bubble surface

$$\rho \ddot{\xi}\Big]_{R=a} = \frac{\sqrt{2}\,\underset{\sim}{P}_s}{R^2}(1-ikR)e^{i(\omega t-kR)}\Big]_{R=a}$$

Since $ka << 1$ this simplifies to

$$|p_s| = \rho\, a\, |\ddot{\xi}| \qquad (1.1.4)$$

The equivalent mass is found by calculating the inertial force at the surface

$$F_m\Big]_{R=a} = - p_s\Big]_{R=a}(4\pi a^2)$$

$$= - 4\pi\, {}^3\rho\, \ddot{\xi}\Big]_{R=a} \qquad (1.1.5)$$

Equation (1.1.5) allows us to identify an effective mass of water

$$m = 4\pi a^3 \rho \qquad (1.1.6)$$

that rides with the bubble as it oscillates at low frequencies, $ka << 1$.

Newton's Second Law is therefore

$$F_r = ma$$

$$\underbrace{- 12\pi\gamma P_o a\xi}_{S_A} = \underbrace{4\pi a^3 \rho}_{m}\ddot{\xi} \qquad (1.1.7)$$

The natural frequency of the free oscillation, f_{RA}, depends only on the constants of the system,

$$f_{RA} = \frac{1}{2\pi}\sqrt{\frac{S_A}{m}} = \frac{1}{2\pi a}\sqrt{\frac{3\gamma P_o}{\rho}} \qquad (1.1.8)$$

The subscript, R, refers to resonance and, A, refers to the mentioned assumption. For an air bubble assumptions in water at sea level pressure this simplifies to

$$f_{RA} = \frac{3.25}{a(\text{meters})} = \frac{3.25 \times 10^6}{a(\text{microns})} \qquad (1.1.9)$$

Defining k_R, the wave number in water at the resonance frequency, the sea level value of $k_R a$ is 0.0136 for an air bubble. This verifies the assumption, $k_R a \ll 1$.

For bubbles of small radii, surface tension becomes a significant additional restoring force. Furthermore, the assumption that the gas vibrates adiabatically is no longer valid if the bubble radius is very small; then the oscillation is more nearly isothermal. When these points are considered, the equation for the resonance frequency changes. P_o in (1.1.8) is replaced by the average interior pressure including surface tension, $P_{io} = \beta P_o$, and γ is replaced by the effective ratio of specific heats in the presence of thermal conductivity γb.
The generalization is

$$f_R = \frac{1}{2\pi a}\sqrt{\frac{3\gamma b \beta P_o}{\rho}} = f_{RA}(\beta b)^{1/2} \qquad (1.1.10)$$

The detailed expressions for b and β will be given later. Figure 1.2 shows their behavior for air bubbles at sea level.

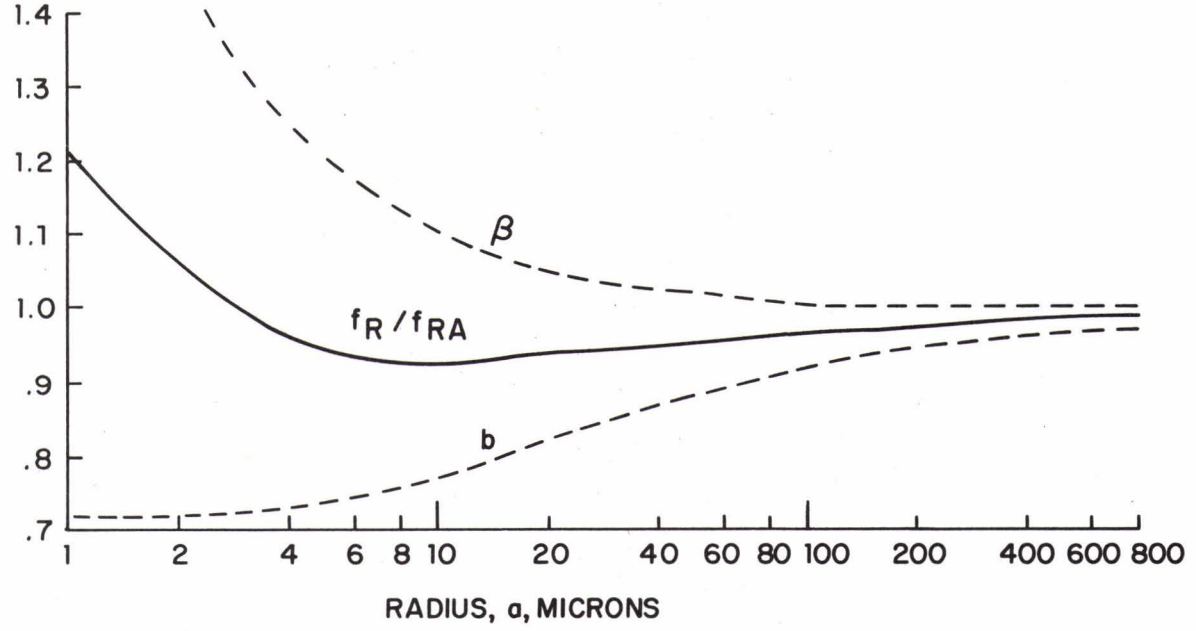

FIG. 1.2
CORRECTIONS TO Eq. 1.1.8 FOR CALCULATION OF BUBBLE RESONANCE FREQUENCY. β AND b ARE GIVEN BY Eqs. (1.1.31) AND (1.1.32) AND ARE PRINCIPALLY FUNCTIONS OF SURFACE TENSION AND THERMAL CONDUCTIVITY, RESPECTIVELY.

The surface tension correction, β, differs from unity by less than 1% for bubbles of radius 100 microns or greater. The thermal conductivity parameter, b, approaches the isothermal value, $1/\gamma$, for very small bubbles and unity for large ones. Fig 1.2 shows that the two effects are to some extent mutually counteracting in their effect on the resonance frequency of bubbles greater than 2 microns, so that the simpler equation (1.1.8) is at worst 8% in error for this case.

1.1.2 Scattering cross section and damping constants

Assume that the bubble is irradiated by a sound field of wave length much greater than the bubble radius ($ka << 1$). The incident plane wave is therefore uniform at all points of the bubble.

$$\underset{\sim}{p}_P = \sqrt{2}\underset{\sim}{P}_P e^{i\omega t} \tag{1.1.11}$$

Where $\underset{\sim}{P}_p$ is the rms incident plane wave pressure. The incident intensity is

$$I_p = \frac{|P_p|^2}{\rho c} \tag{1.1.12}$$

From (1.1.3) the scattered intensity is

$$I_S = \frac{|P_S|^2}{R^2 \rho c} \tag{1.1.13}$$

The scattering cross section is the ratio of the scattered power to the incident intensity,

$$\sigma_s = \frac{\int_A I_S dA}{I_P} = \frac{4\pi R^2 \dfrac{|P_S|^2}{R^2 \rho c}}{\dfrac{|P_P|^2}{\rho c}} = 4\pi \frac{|P_S|^2}{|P_P|^2} \tag{1.1.14}$$

To determine the pressure ratio in eq (1.1.14) express the pressure and particle velocity boundary conditions at the bubble surface. Denote the interior acoustic pressure by

$$\underset{\sim}{p}_i = \sqrt{2}\underset{\sim}{P}_i e^{i\omega t} \tag{1.1.15}$$

where $\underset{\sim}{P}_i$ is the rms interior pressure.

In addition to the pressures given by Eqs (1.1.3), (1.1.11) and (1.1.15) we must add a shear viscous stress proportional to the radial rate of strain, u_r/R at the surface. The proportionality constant, $C_1\mu$, includes the dynamic coefficient of shear viscosity for water, μ, and the dimensionless constant, C_1, which depends on the geometry.

The boundary condition for pressure is

$$p_i = p_p + p_s + C_1\mu \left.\frac{u_r}{R}\right]_{R=a} \tag{1.1.16}$$

To obtain u_r in terms of the scattered pressure use the radial component of the acoustic force equation at the surface,

$$\rho \left.\frac{\partial u_r}{\partial t}\right]_{R=a} = -\left.\frac{\partial p_s}{\partial R}\right]_{R=a}$$

Assuming harmonic time dependence for u_r,

$$\underset{\sim}{u}_r = \frac{-i\sqrt{2}\,\underset{\sim}{P}_S\, e^{i\omega t}}{\rho c k a^2} \tag{1.1.17}$$

To obtain p_s at R = a expand the exponential in Eq (1.1.3),

$$\underset{\sim}{P}_S = \frac{\sqrt{2}\,\underset{\sim}{P}_S}{a}\, e^{i\omega t}(1-ika) \tag{1.1.18}$$

Inserting these results into (1.1.16), the pressure condition at R = a is

$$\underset{\sim}{P}_i = \underset{\sim}{P}_P + \frac{\underset{\sim}{P}_S}{a}(1 - ika) - \frac{i\mu C_1 \underset{\sim}{P}_S}{\rho c k a^3} \tag{1.1.19}$$

Next turn to the velocity condition. The interior radial particle velocity at the surface can be evaluated in terms of the alternating pressure, $\underset{\sim}{p}_i$. First, consider the relation between the bubble volume and the interior pressure.

For small bubbles the effective value of the ratio of specific heats, γ, approaches unity. Of equal importance, the interior bubble pressure and temperature do not instantly follow the volume variation. Therefore, rewrite the adiabatic law to allow the magnitude of the exponent and the phase between pressure and volume to be functions of driving frequency and bubble size,

$$\underset{\sim}{p}_{iT} \, V^{\gamma(b+id)} = \text{constant} \tag{1.1.20}$$

where

$$\underset{\sim}{p}_{iT} = P_{io} + \underset{\sim}{p}_{i} = \text{total interior pressure.} \tag{1.1.21}$$

b and d are real dimensionless numbers. Differentiate with respect to time, use

$$\frac{d\underset{\sim}{V}}{dt} = 4\pi a^2 \, \underset{\sim}{u}_r \Big]_{R=a} \tag{1.1.22}$$

and

$$u_r \Big]_{R=a} = \frac{-i\omega a \sqrt{2} \, P_i \, e^{i\omega t}}{3\gamma(b+id) P_{io}} \tag{1.1.23}$$

Equate to the particle velocity of the radiated wave at R = a, given by (1.1.17), rearrange to

$$\frac{\underset{\sim}{P}_i}{\underset{\sim}{P}_S} = \frac{3\gamma(b+id) P_{io}}{\rho c^2 k^2 a^3} \tag{1.1.24}$$

which, with the aid of (1.1.10), can be written

$$\frac{\underset{\sim}{P}_i}{\underset{\sim}{P}_S} = \frac{1}{a}\left(\frac{f_R}{f}\right)^2\left(1 + id/b\right) \tag{1.1.25}$$

Also, since eqs (1.1.17) and (1.1.23) show that $\underset{\sim}{u}_r$ lags $\underset{\sim}{p}_s$ by 90° and leads $\underset{\sim}{p}_P$ by 90°, when evaluated at R = a and f << f_R, we replace $\underset{\sim}{P}_p$ by - P_p. This effectively fixes the phase in terms of the incident wave as reference. Then

$$\frac{\underset{\sim}{P}_S}{P_P} = \frac{-a}{\left[\left(\frac{f_R}{f}\right)^2 - 1\right] + i\left[ka + \left(\frac{d}{b}\right)\left(\frac{f_R}{f}\right)^2 + \frac{C_1\mu}{\rho\omega a^2}\right]} \tag{1.1.26}$$

Now define the damping constants

$$\delta = \delta_r + \delta_t + \delta_v \tag{1.1.27}$$

where

δ_r = ka is the damping constant due to reradiation;

$\delta_t = (d/b)(f_R/f)^2$ is the damping constant due to thermal conductivity;

and $\delta_v = \frac{4\mu}{\rho\omega a^2}$ is the damping constant due to shear viscosity.

Our proportionality constant C_1 has been given the value 4, as found in other studies (Devin 1959).

The scattering cross section is obtained by inserting (1.1.26) into (1.1.14)

$$\sigma_S = 4\pi\frac{\underset{\sim}{P}_S\underset{\sim}{P}_S^*}{P_P} = \frac{4\pi a^2}{\left[\left(\frac{f_R}{f}\right)^2 - 1\right]^2 + \delta^2} \tag{1.1.28}$$

It is clear that at resonance the values of δ are crucial to the size of the scattering cross section. The damping constants have been evaluated in terms of the physical constants of the gas bubble and water. (Ref. Eller, A.I. (1970) and Devin, C. (1959)). In referring to the above articles note that Devin is principally concerned with the damping constants at resonance and that Eller's damping constants are related to ours by $d(\text{eller}) = \delta(f/f_R)^2$.

In order to obtain δ_t, the thermal damping constant, calculate

$$d/b = 3(\gamma-1)\left[\frac{X(\sinh X + \sin X) - 2(\cosh X - \cos X)}{X^2(\cosh X - \cos X) + 3(\gamma-1)X(\sinh X - \sin X)}\right], \quad (1.1.29)$$

where

$$X = a\left(\frac{2\omega\rho_g C_{Pg}}{K_g}\right)^{1/2} \quad (1.1.30)$$

The constants needed for the resonance frequency equation, (1.1.10), are

$$\beta = P_{io}/P_o = 1 + \frac{2\tau}{P_o a}\left(1 - \frac{1}{3\gamma b}\right) \quad (1.1.31)$$

and

$$b = \left[1 + (d/b)^2\right]^{-1}\left[1 + \frac{3(\gamma-1)}{X}\left(\frac{\sinh X - \sin X}{\cosh X - \cos X}\right)\right]^{-1} \quad (1.1.32)$$

In summary, to calculate the resonance frequency and the damping constants, the procedure is: Obtain the physical constants of the bubble at the depth, Z ; this will include the constants of the gas, ρ_{gO}, K_g, C_{pg}, γ, the constants of the water, ρ ,μ and the surface tension between them, τ. For a given sound frequency and bubble radius calculate X, and then d/b, b and β in that order. The resonance frequency for that bubble radius can then be obtained from eq (1.1.10) and the damping

constants readily fall out of equations (1.1.27). The damping constants at resonance are shown in Fig 1.3

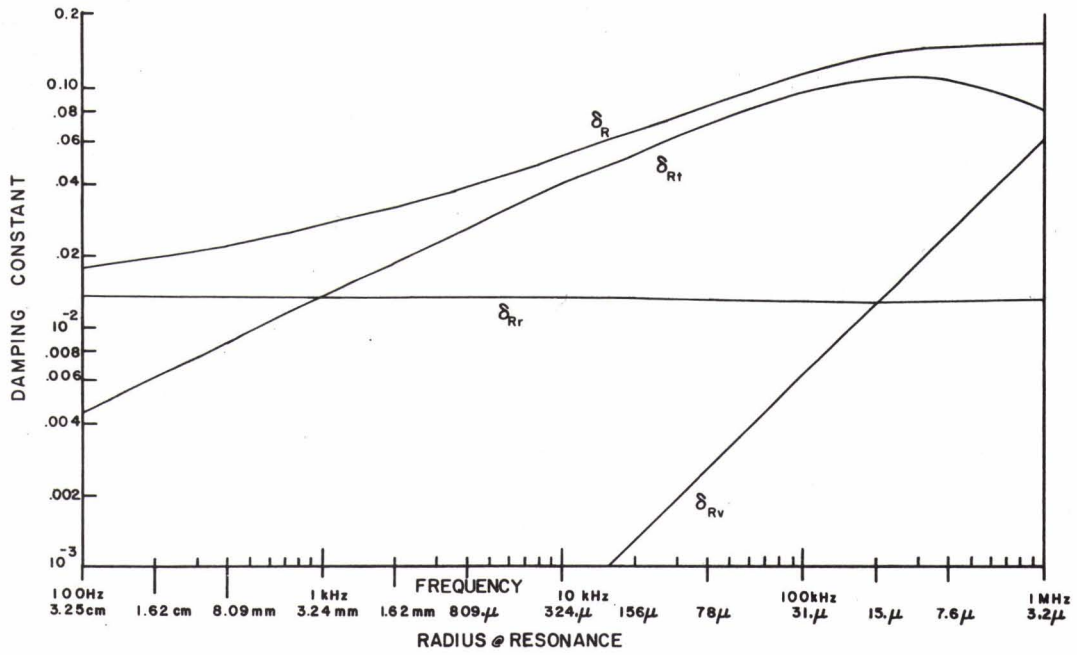

FIG. 1.3
DAMPING CONSTANTS AT RESONANCE, δ_{Rt}, δ_{RV} AND δ_{Rr} ARE COMPONENTS DUE TO THERMAL CONDUCTIVITY, SHEAR VISCOSITY AND SCATTER

In order to calculate the acoustical cross sections it is necessary, also to look at the damping constants off-resonance. Fig 1.4 shows the damping constants of bubbles as a function of radius at frequencies 1, 10, 100 kHz. The resonance radius, a_R, is indicated. Fig 1.4 (next page) shows that the damping constant for a given sound frequency is dominated by different mechanisms depending on the bubble radius. For $a >> a_R$, δ depends principally on scatter, (δ_r), and is proportional to the radius (see eq 1.1.27); bubbles near, and down to two decades smaller than, the resonance radius have damping constants largely caused by thermal conductivity; very small bubbles $a << a_R$ have large damping constants proportional to a^{-2} due solely to shear viscous losses. The minimum damping constant occurs at radius $a_{min} > a_R$; the ratio a_{min}/a_R increases with increasing frequency.

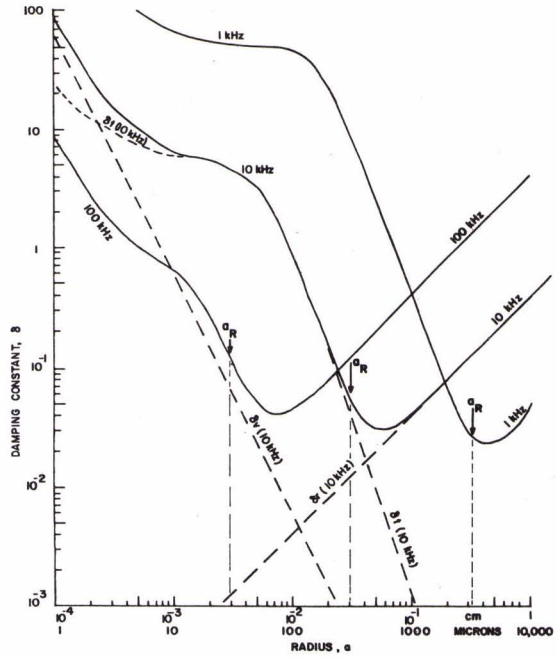

FIG. 1.4
DAMPING CONSTANTS OFF RESONANCE. RESONANCE RADII ARE INDICATED

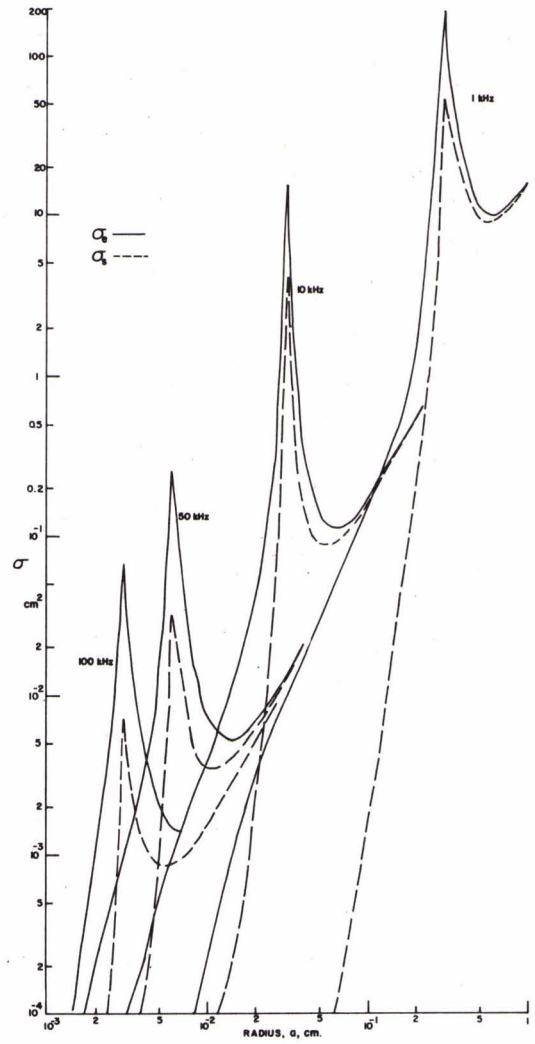

FIG. 1.5
σ_e AND σ_s FOR AIR BUBBLES AT SEA LEVEL

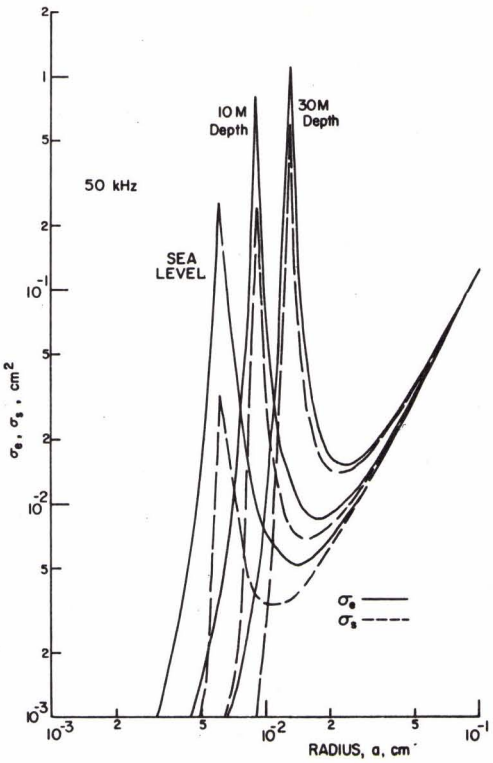

FIG. 1.6
σ_e AND σ_s FOR AIR BUBBLES AT THREE DEPTHS. f = 50 kHz

Fig 1.5 shows σ_s and σ_e as a function of bubble radius for air bubbles at sea level, ensonified by 1, 10, 50 and 100 kHz sound. In Fig 1.6 σ_s and σ_e are plotted for 50 kHz sound for bubbles at different depths. σ_e will be discussed in the next section.

1.1.3 Absorption and extinction cross sections

The extinction cross section of a bubble can be calculated from

$$\sigma_e = \Pi_e / I_p \tag{1.1.37}$$

where Π_e is obtained by integrating the product of the force by the velocity, at R = a,

$$\Pi_e = \frac{1}{T} \int_T (\underset{\sim}{p}_p)(4\pi a^2)(\underset{\sim}{\dot{\xi}})\, dt \Big]_{R=a} \tag{1.1.38}$$

We readily get

$$\sigma_e = \frac{\Pi e}{P_p^2/\rho c} = \frac{4\pi a^2 (\delta/ka)}{[(f_R/f)^2 - 1]^2 + \delta^2} \tag{1.1.39}$$

Comparison of the equations for scatter and extinction make it clear that

$$\sigma_e = \sigma_s (\delta/\delta_r) \tag{1.1.40}$$

Also, since sound extinction is composed of scatter plus absorption,

and $$\sigma_e = \sigma_s + \sigma_a, \tag{1.1.41}$$

we have

$$\sigma_a = \sigma_s \left(\frac{\delta_t + \delta_v}{\delta_r} \right) \tag{1.1.42}$$

Recall that δ_t and δ_v measure true sound absorption whereas δ_r measures scatter out of the beam. Therefore, the last two equations state that the cross sections are directly proportional to the particular damping constants that cause them.

1.2 Homogeneous Bubbly Water

1.2.1 Attenuation

a) Bubbles of one size only: Assume that we have water containing bubbles of unique radius, a, and that the bubbles are far enough apart to prevent interaction effects. Effectively this will be true when the separation is greater than $\sqrt{\sigma_e}$. If a sound beam propagates through such a medium the excess attenuation due to bubbles can be obtained by simply adding the extinction effect of each bubble. Assuming N resonant bubbles per unit volume, the change of intensity over a distance dx is

$$dI = I_p \sigma_e N(a) dx$$

The excess attenuation in decibels per unit distance due to bubbles will be

$$\alpha_b = \frac{\Delta SPL}{x} = 4.34 \sigma_e N(a) \qquad (1.2.1)$$

where the length units must be consistent, e.g.,

$$[\sigma_e] = M^2 \ , \ [N(a)] = M^{-3}, \ [\alpha] = dB/M$$

b) Bubbles of Many Sizes: At sea there will be a mixture of bubbles sizes. The total extinction cross section per unit volume, S_e, for sound traversing a random mixture of non-interaction of bubbles is calculated by integration

$$S_e = \int_0^\infty \sigma_e n(a) da = \int_\delta^\infty \frac{4\pi a^2 (\delta/\delta_r) n(a) da}{[(f_R/f)^2 - 1]^2 + \delta^2} \qquad (1.2.2)$$

where n(a) da is the number of bubbles per unit volume having a radius between a and a+ da.

When Eq 1.2.2 is integrated (Eckart 1945) by assuming that both δ_R and n(a) da are constant over the major part of the resonance peak,

$$S_e = 2\pi^2 a_R^3 \frac{n(a_R)}{\delta_{Rr}}$$

which replaces σ_e N in eq 1.2.1.

Accordingly the excess attenuation due to bubbles is estimated as

$$\alpha_b = 8.68 \ \pi^2 \ \frac{a^3_R}{\delta_{Rr}} n(a_R) = \frac{20.5 \ u(a_R)}{\delta_{Rr}} \qquad (1.2.3)$$

where u(a)da is the ratio of bubble gas volume to water volume for bubbles between radius a_R and $a_R + da_R$. That is,

$$u(a_R)da_R = [\frac{4}{3}\pi a_R^3]n(a_R)da_R$$

1.2.2 Dispersion of sound speed

a) Bubbles of One Size Only: The dependence of the sound speed on the compressibility and density is given by

$$c^2 = E/\rho = \frac{1}{\rho K}$$

where the compressibility is the reciprocal of the bulk elasticity,

$$K = \frac{1}{E} = \frac{\Delta\rho/\rho}{\Delta\rho} = \frac{|\Delta v/v|}{\Delta P} = K_o + \underset{\sim}{K}_1 \qquad (1.2.4)$$

The presence of bubbles in sea water affects the speed of sound primarily because of the changed compressibility. K_o is the part of the compressibility due to the water and $\underset{\sim}{K}_1$ is the part due to the change in volume of the bubbles. $\underset{\sim}{K}_1$ is written as a complex quantity to allow for the phase shift of volume change with respect to pressure change.

K_o is expressed in terms of the speed of sound through bubble-free water, c_o, and the density, ρ_o,

$$K_o = \frac{1}{\rho_o c_o^2} \qquad (1.2.5)$$

The compressibility due to the bubbles is found by using the displacement from eq (1.1.34) in (1.2.4)

$$\underset{\sim}{K}_1 = \frac{N\underset{\sim}{\Delta v}}{\Delta P} = \frac{NS\underset{\sim}{\xi}}{\sqrt{2}\, p_p e^{i\omega t}} = \frac{NS^2}{m\omega^2[(-1+\frac{\omega_R^2}{\omega^2})+i\frac{R_m}{\omega m}]} \qquad (1.2.6)$$

where

N is number of bubbles of radius, a, per unit volume, Δv is change in volume for each bubble, $S = 4\pi a^2$ is surface area of each bubble and $\underset{\sim}{\xi}$ is radial displacement of bubble surface. To simplify we define the frequency ratio

$$Z = f_R/f = \omega_R/\omega \qquad (1.2.7)$$

Then,

$$\underset{\sim}{K}_1 = \frac{N4\pi a[Z^2-1-i\delta]}{\rho_o\omega^2[(Z^2-1)^2+\delta^2]} \qquad (1.2.8)$$

The expression for the speed of sound in the bubbly medium is now

$$\underset{\sim}{c} = \left(\frac{1}{\rho_o \underset{\sim}{K}}\right)^{1/2} = \frac{c_o}{[1+A-iB]^{1/2}} \qquad (1.2.9)$$

where

$$A = \left(\frac{Z^2-1}{(Z^2-1)^2+\delta^2}\right)\left(\frac{4\pi a N c_o^2}{\omega^2}\right) \text{ and } B = \left(\frac{\delta}{(Z^2-1)^2+\delta^2}\right)\left(\frac{4\pi a N c_o^2}{\omega^2}\right)$$

Take the real part of $\underset{\sim}{c}$ for the dependence of the speed on the parameters of the bubbly region.

$$\mathrm{Re}\{\underset{\sim}{c}\} = c_o\left[1 - \frac{2\pi a N c_o^2}{\omega^2}\,\frac{(Z^2-1)}{(Z^2-1)^2+\delta^2}\right] \qquad (1.2.10)$$

It is useful to write the speed in terms of the fraction of gas in bubble form, U(a),

$$U(a) = [N(a)]\left[\tfrac{4}{3}\pi a^3\right] \qquad (1.2.11)$$

Then,

$$\mathrm{Re}(\underset{\sim}{c}) = c_o\left[1 - \frac{3UZ^2}{2a^2k_R^2}\,\frac{Z^2-1}{(Z^2-1)^2+\delta^2}\right] \qquad (1.2.12)$$

Where $k_R = \omega_R/c_o$

Consider the special cases for extreme frequencies. For $Z \gg 1$,

$$c_{\ell f} = c_o\left[1 - \frac{3U}{2a^2k_R^2}\right] \quad f \ll f_R, \qquad (1.2.13)$$

so that the low frequency asymptotic speed depends only on the total gas volume.

At the other extreme for $Z << 1$

$$c_{hf} = c_o \left[1 + \frac{3UZ^2}{2a^2 k_R^{\ 2} (1+\delta^2)} \right] \rightarrow c_o \quad \cdot \quad f >> f_R \tag{1.2.14}$$

Therefore bubbles do not affect the sound phase speed if the frequency is high enough. Sound velocimeters, which operate in the megahertz range, provide values of c_o, even in bubbly water because $f >> f_R$ for the significant fractions U(a).

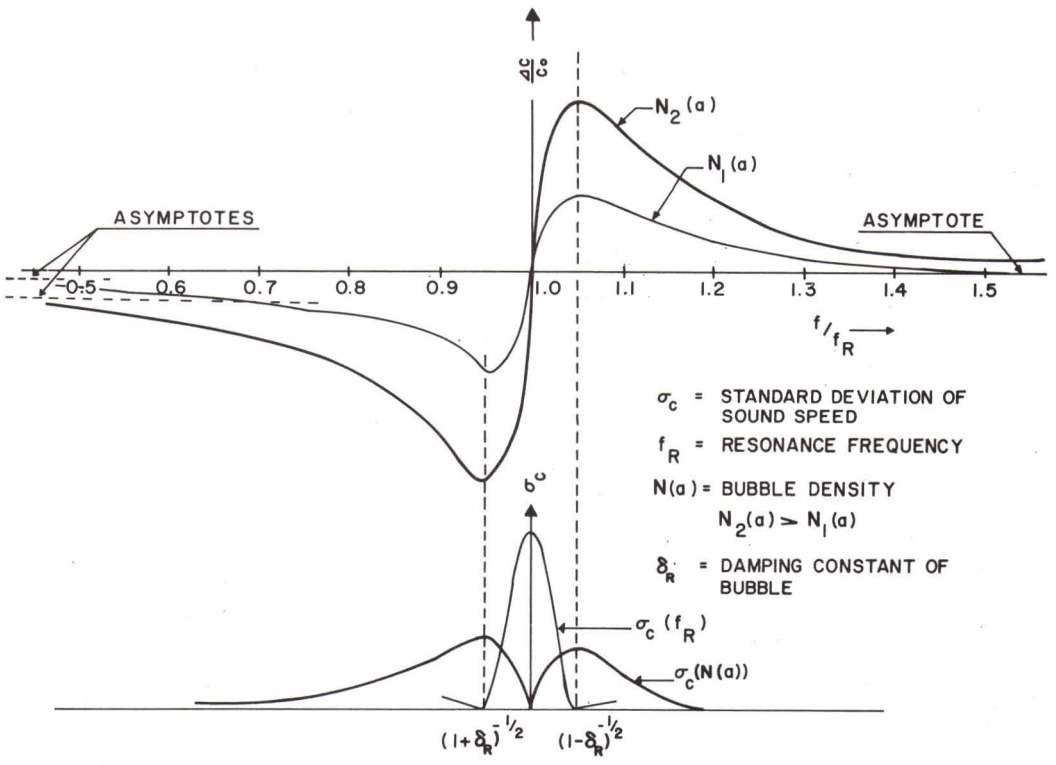

FIG. 1.7
UPPER GRAPH: FRACTIONAL CHANGE OF SPEED OF SOUND FOR A BUBBLY MEDIUM OF ONE BUBBLE RADIUS, a. LOWER GRAPH: STANDARD DEVIATION OF FLUCTUATIONS IN SPEED OF SOUND DUE TO CHANGE OF NUMBER OF BUBBLES PER UNIT VOLUME, $\sigma_c[\ N(a)\ ]$, AND DUE TO CHANGE OF RESONANCE FREQUENCY WITH A CONSTANT NUMBER OF BUBBLES, $\sigma_c(f_R)$

Fig 1.7 shows the dispersion for a bubble resonance frequency, 65 kHz, at which $\delta_R \simeq 0.1$. The abscissa is $z^{-1} = f/f_R$. The ordinate is the fractional change in speed, in units of the fractional change at low frequencies. The maximum and minimum occur at frequencies given approximately by $f = f_R\,(1 \pm \delta_R/2)$. The speeds at these points differ from that in bubble-free water by approximately

$$\pm \frac{1}{2\delta_R}\left(\frac{3U}{2a^2k_R^{\,2}}\right).$$

b) Bubbles of Many Sizes:

The generalization to a bubbly medium of random radii is accomplished by replacing N(a) by n(a) da and U(a) by u(a)da. Because all contributions to the compressibility are very small quantities, they add linearly and the speed of sound in the bubbly region can be written

$$\mathrm{Re}\{\underset{\sim}{c}\} = c_o\left[1 - \frac{3}{2}\int_{a_i}\frac{u(a_i)z_i^{\,2}(z_i^{\,2}-1)\,da_i}{a_i^{\,2}k_{iR}^{\,2}[(z_i^{\,2}-1)^2+\delta_{iR}^{\,2}]}\right] \qquad (1.2.15)$$

The effect of a mixture of bubble sizes is to smear the dispersion curve so that although the magnitudes of the deviation from the bubble-free value are increased, the frequency range between the peak and the trough is also increased.

2. Ocean Experiments

Good agreement between theory and experiment for clean laboratory bubbles has encouraged acoustical exploration for bubbles at sea.

In-situ bubble research has been done with equipment sketched in Fig 2.1a (Medwin 1970) and 2.1b (Medwin et al 1975)

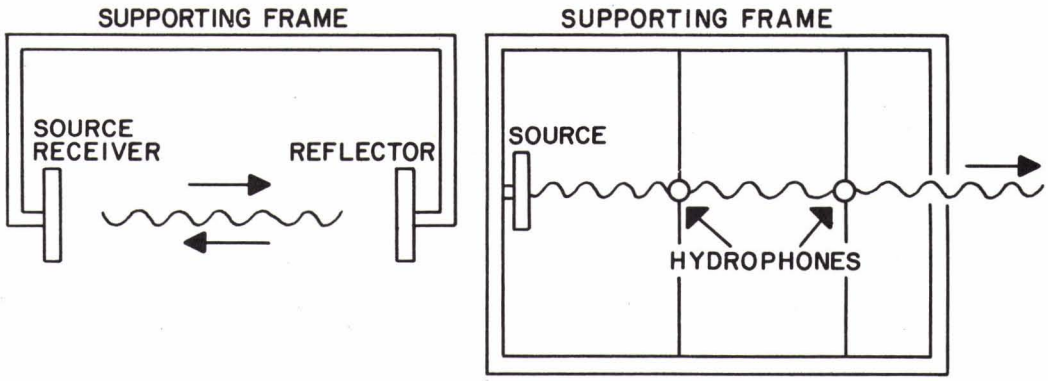

FIG. 2.1
TWO EXPERIMENTAL SCHEMES FOR MEASURING BUBBLE EFFECTS AT SEA:
LEFT: PULSE-ECHO TECHNIQUE; RIGHT: c.w. TECHNIQUE

The devices are generally 2 to 7 meters in extent, and are constructed so that the water medium freely enters the ensonified space.

2.1 Pulse-echo technique

In the pulse-echo technique a sinusoidal wave train of duration approximately 0.5 msec has been used with the transducer electronically switched to receive the reflected echoes. The oscilloscope screen was photographed to record the echo patterns (Fig 2.2).

In principle a single oscillogram may be analyzed in three different ways to obtain the variables of the medium: (1) comparison of the exponential attenuation shown by the echo pattern at sea with that in clean water provides the excess absorption and scattering by objects (assumed to be bubbles) at sea; (2) the relative reverberation between echoes,

compared to the preceding and following echo levels, measures the scatter due to bubbles along the path; (3) the time between echoes permits a calculation of the local speed of propagation. In practice, because of phase shift at the reflectors, the sound speed dispersion due to bubbles at sea has been too small to measure accurately with our pulse-echo system. However, we have determined the extinction cross sections and the scattering cross sections, as a function of frequency at sea. By using both the extinction and the scatter data the absorption cross section can be found and the number of bubbles in a given radius increment per unit volume of water is directly calculable. We assume that the scattering and absorption cross sections of dirty gas bubbles are approximately the same as for clean bubbles.

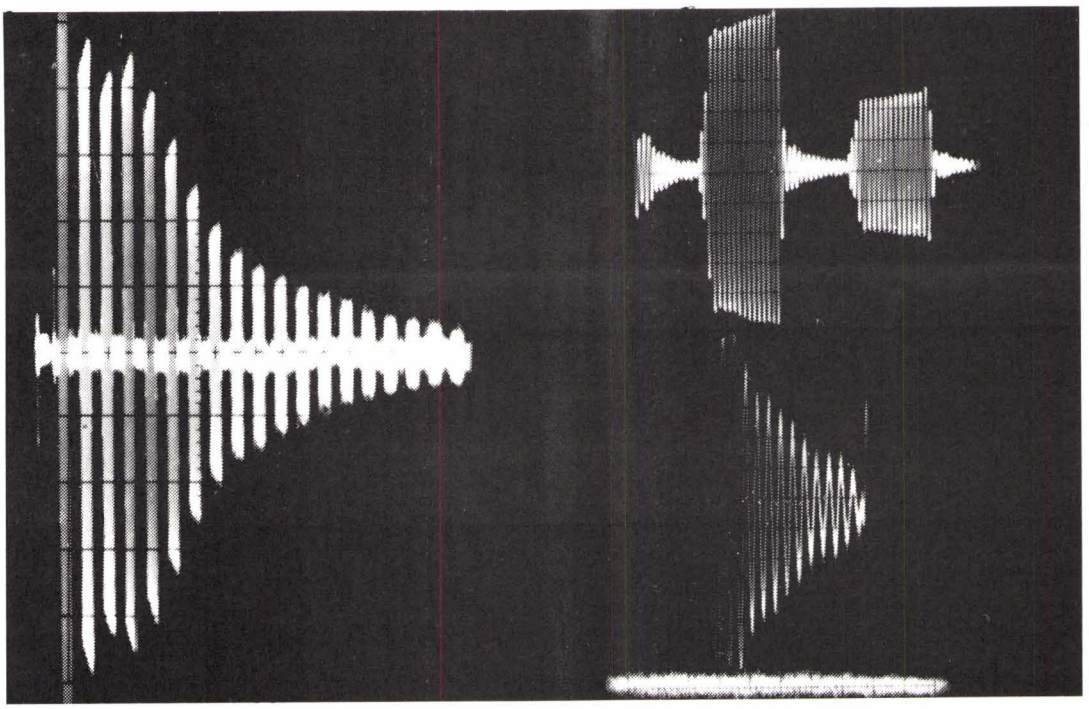

FIG. 2.2
LEFT: OSCILLOGRAM SHOWING 19 ECHOES OF A PULSE-ECHO PATTERN AT 200 kHz. RIGHT: TOP, TWO ECHOES AND BACKSCATTER BETWEEN THEM AT 30 kHz; MIDDLE, AMPLIFIED BACKSCATTER BETWEEN TWO ECHOES; BOTTOM, SYSTEM NOISE LEVEL ON SAME SCALE AS BACKSCATTER

2.2 Continuous wave technique

It is also possible to obtain in-situ bubble information by continuous wave acoustic measurements. (Medwin et al 1975). The study requires only the sound source and two point hydrophones separated by a fixed distance (Fig 2.1) .

The speed is easily found as a function of frequency by measuring the number of wavelengths between the two hydrophones. Then,

$$c = f\lambda = f \frac{x}{M + \phi/360} \qquad (2.1.1)$$

where x is the distance between the two hydrophones, M + Ø/360 is the integral plus fractional number of wave lengths. The number, M, is obtained by using a rough value of the bubble-free speed, c_o, or from a sound velocimeter. A good phasemeter can give Ø to the nearest tenth of a degree. f is known to 1 part in 10^6 by using a frequency synthesizer or stable oscillator and frequency counter. In fact it is the measurement of distance, x, that is the crudest part of the experiment and that limits the absolute accuracy if the high frequency calibration is not used.

The same cw equipment may be used to measure the attenuation between the two hydrophones and, thereby, to assess the bubble density or volume fraction in particular bands of bubble radii. The attenuation can be found by either analogue or digital measurements. Recently we have been analyzing the simultaneous digital time series from the two hydrophones by FFT. This provides both magnitude and phase of the signal at each of the two hydrophones. The ratio of the magnitudes then gives the attenuation. The difference of the phases, used in eq 2.1.1, yields the speed. When a harmonic-rich signal is used for the sound source, both the attenuation and phase shift can be determined, from the same data for a large number of frequencies (Huffman and Zveare 1974). The mini-computer that we use can do the A/D conversion for the two series at rates up to 320 kHz for each channel simultaneously. Therefore, by using 5 kHz sawtooth input we are able to get speeds and attenuations for the 32 harmonics up to 160 kHz.

3. Acoustically Inferred Bubble Populations at Sea

3.1 Assumptions in an acoustical determination

Our conversion from attenuation or dispersion measurements to bubble populations assumes the constants of the physicist's clean, free, air bubble. But bubbles at sea are of other gases, as well as air, and they may have organic skins or other detritus on their surfaces, or, indeed, be parts of phyto-plankton or zoo-plankton. The inferred radius will be affected by these changed conditions, but in no major way. For example, realistic ocean bubble gases include oxygen, carbon dioxide, carbon monoxide, hydrogen sulfide and methane for which the value γ ranges from 1.30 to 1.40. The error in the resonance radius assuming air, instead of the true gas, would be at most 5% according to eq (1.18).

On the other hand, changing bubble gas from air to methane or carbon dioxide, for example, results in a significant increase in σ_e and σ_s because of the different damping constants. At 50 kHz, a sea level bubble at resonance has $\sigma_e = 0.40$ cm^2 if it is of air, whereas it is 0.46 cm^2 for CH_4 and 0.60 cm^2 for CO_2. For the same conditions, σ_s is 0.056 cm^2 for the air bubble, 0.074 cm^2 for CH_4 and 0.13 cm^2 for CO_2. Not knowing the bubble gas thereby degrades the accuracy of the acoustical determination of bubble populations by extinction or backscatter experiments alone.

Since $\sigma_e = \sigma_a + \sigma_s$, and since σ_s increases with bubble radius (see $a > a_R$ in Figs 1.5, 1.6) in spite of the high Q character of the cross sections at resonance the variation of bubble number with bubble radius could conceivably affect its very determination. Fortunately, absorption measurements in tap water (Gavrilov, 1969) and our own work at sea show that the variation of $n(a)da$ with radius lies between a^{-4} and a^{-2}. Under these conditions the integration of eq (1.2.2) converges and the resonance peak, alone, can be used to calculate the bubble density at that resonance radius. It is for this reason that excess attenuation or backscatter data obtained as a function of frequency can be interpreted as bubble radius spectrometry.

Measurements in the near-surface ocean, where bubbles are common, do not produce constant values. This is partly because of the inhomogeneity of the medium and partly because of the orbital motion associated with surface waves. Our selection of a one meter path between the two hydrophones fixes our averaging space for the inhomogeneous ocean. In our

analog work we use an averaging time of 10 to 20 minutes for each frequency. In our digital work, a run takes only 3.2 ms and the temporal variations as well as the averages are identified by repeated measurements.

3.2 Bubble fractions and bubble densities.

Our first ocean bubble experiments were done at the NUC Oceanographic Tower, off San Diego, about 10 years ago. (Medwin 1970). Since that time we have made measurements in BASS Strait, Australia (Medwin et al 1975) and most recently in Monterey Bay (Huffman and Zveare 1974). Nevertheless we feel as innocent in this vastly complicated study as the propagation people must have felt when the first bathythermograph was obtained in the 1930's. What we can say is this: Bubble densities decrease with greater depth; they increase with greater wind speeds; small bubbles are apparently greater in number in the day time than at night, however, for bubbles larger than about 60μ the opposite is true. But this is about all that we have the courage to say at this time.

Figs 3.1 - 3.4 are samples of what we find. This particular case from the MS Thesis of Huffman and Zveare (1974) was observed 0.9 nautical miles from shore, using the research vessel ACANIA at anchor in water of depth 38M on 12-13 November 1974. The wind speed was 2 knots, cloud cover was 25 to 80%, and the ship was surrounded by "thousands" of squid. The data represent averages of 5 runs taken over 15 minutes. At 1630 on 12 November strong attenuations were observed at 15 kHz and 40 kHz. These attenuations are greater, nearer the surface (Fig 3.1) and the predominant bubble populations that they represent are confirmed by the characteristic dispersion shapes at these same frequencies in Fig 3.2. The inferred bubble populations plotted in Fig 3.3 present the typical a^{-4} slope for $f < 60\mu$ and a^{-2} for $f > 60\mu$, that we have consistently seen. Fig 3.4 shows the dependence on time of day; the larger bubbles were somewhat more common at night (sunset was at 1700, sunrise at 0645).

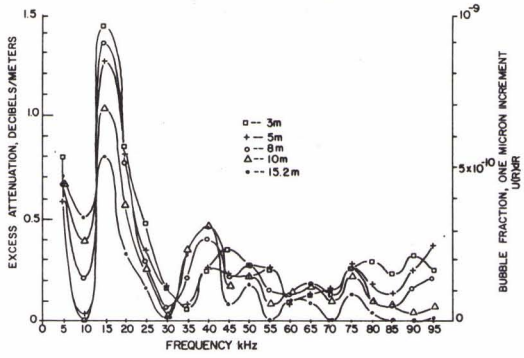

FIG. 3.1
EXCESS ATTENUATION DUE TO BUBBLES AT FIVE DEPTHS, 12 NOV 1974
HUFFMAN AND ZVEARE, 1975

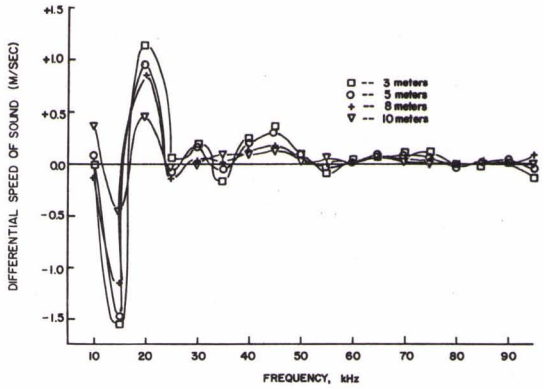

FIG. 3.2
SOUND SPEED DISPERSION AT FOUR DEPTHS, 12 NOV 1974
HUFFMAN AND ZVEARE, 1975

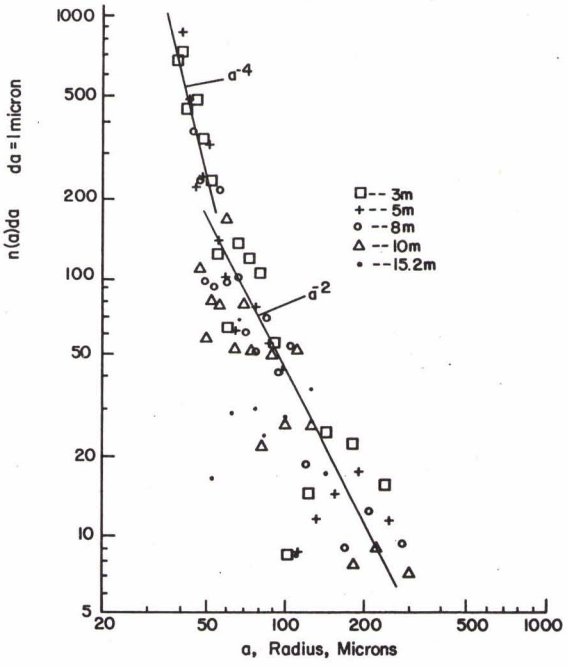

FIG. 3.3
NUMBER OF BUBBLES PER CUBIC METER IN A ONE MICRON RADIUS INCREMENT FROM DATA OF FIG. 3.1
HUFFMAN AND ZVEARE, 1975

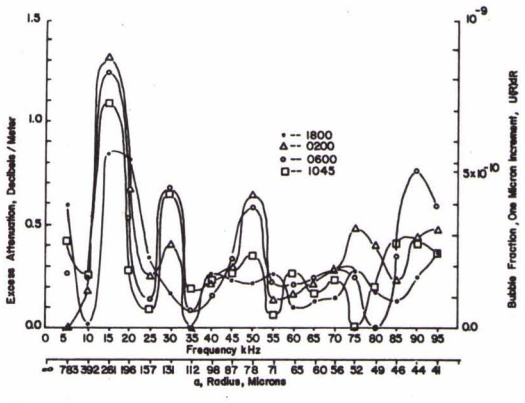

FIG. 3.4
EXCESS ATTENUATION AT 5 m DEPTH AT DIFFERENT TIMES OF DAY. 12, 13 NOV 1974
HUFFMAN AND ZVEARE, 1975

4. Fluctuations due to Bubbles

Sound-speed measurements as a function of frequency, not only reveal bubble presence but they also show that the principal cause of sound-phase fluctuations near the sea surface can be bubble presence rather than temperature microstructure.

Three major sources of speed fluctuations due to bubbles have been identified (Medwin 1974):

(1) Change of speed can be caused by change of total volume fraction of bubbles. From Eq 1.2.13 note that at frequencies well below resonance, change of total volume fraction U causes the variance

$$\mathrm{Var}\{c(U)\} = \left(\frac{3c_o}{2a^2 k_R^2} \right)^2 \mathrm{Var}\{U\}, \quad f \ll f_R \qquad (4.1.1)$$

(2) For a single or predominant bubble radius, it has been determined (Wang and Medwin 1974) that change of number of bubbles will cause peak variances at the frequencies of the speed maximum and minimum given by

$$Z = (1 \pm \delta_R/2).$$

The effect causes peak variances

$$\mathrm{Var}\{c[u(a)]\} = \left[\frac{3c_o(1 \pm \delta_R)}{4a^2 k_R^2 \delta_R} \right]^2 \mathrm{Var}\{u(a)\}. \qquad (4.1.2)$$

The (+) sign, giving the larger variance, occurs at the frequency below resonance. See Fig 1.7.

(3) For a single, or predominant, bubble radius in a distribution, a change of ambient pressure will change the resonance frequency and thereby cause a variation in speed. This effect is also shown in Fig 1.7, where it is identified as producing an rms change $\sigma_c(f_R)$. The magnitude of the effect has been derived and is

$$\mathrm{Var}\{c(Z)\} = \left\{ \frac{Bu(a)\,da\,c_o}{(k_R a)^2 [1 + (D/10)\delta_R^2]} \right\}^2 \mathrm{Var}\{h\} \exp(-2\kappa_0 D),$$

Where $B = 0.083M^{-1}$, Var{c(Z)} is the variance of fluctuations in sound speed due to perturbations of bubble resonance frequency, Var{h} is the variance of height of surface waves in square meters and D is the experiment depth in meters, and K_o is the surface wave number.

An experimental way to distinguish between the three bubble sources of sound-speed variation is by correlation or spectral analysis. (H. Medwin et. al (1975)). For example, in the BASS Strait experiment, at a frequency 24.4 kHz, which is low enough to be essentially unaffected by any specific bubble resonance, the autospectrum of the phase variations is close to Gaussian because of its wide-band random nature (Fig 4.1). But near a predominant bubble resonance frequency, models (2) and (3) are appropriate. Since the frequencies for the two effects are very close it is the magnitude of the cross-correlation with wave height that is the clue to model (3). A particularly large cross correlation was found at frequency 95.6 kHz. Three typical spectra of the fluctuations of sound phase are shown in Figure 4.1. In comparison with 95.6 kHz, all of the spectra for sound frequency 24.4 kHz are flatter and closer to a Gaussian form. They also have near-Gaussian correlation functions and large values of σ_U/U.

On the other hand, the predominant feature of the phase fluctuations for 95.6 kHz is the strong peak at the ocean surface wave peak frequency of 0.17 Hz. All spectra for 95.6 kHz showed this peak which decreased in magnitude with increasing depth. In Figure 4.2 some of the data have been plotted on log-log scale in order to show the power law dependence on frequency. The phase fluctuation spectrum is almost a twin to the ocean surface wave spectrum as it follows the F^{-5} law that would be expected [Phillips, 1966] for a fully-developed sea. The modulation spectral density at 0.3 Hz has been selected to plot against depth (not shown). The slope, which turns out to be approximately exp(-D/4.7 m), is an alternative way to determine the depth dependence of predominant bubble populations.

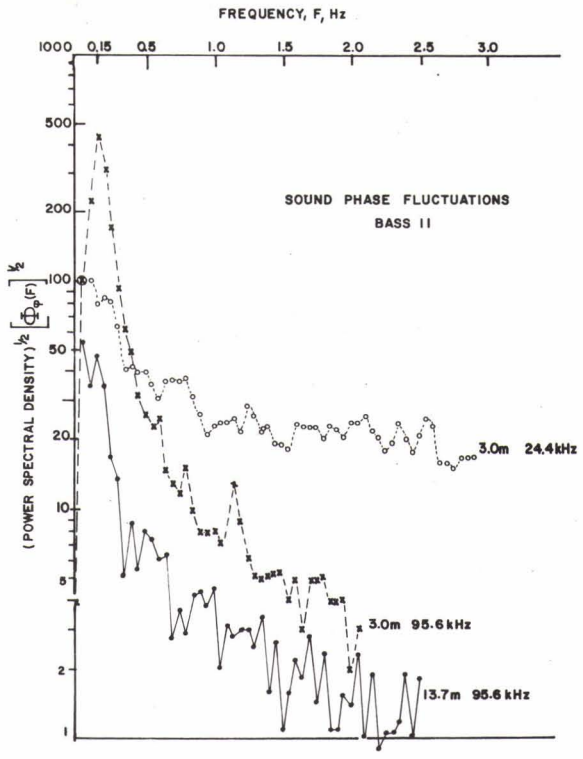

FIG. 4.1
FREQUENCY SPECTRA OF SOUND PHASE FLUCTUATIONS AT 24.4 AND 95.6 kHz DURING BASS EXPERIMENT

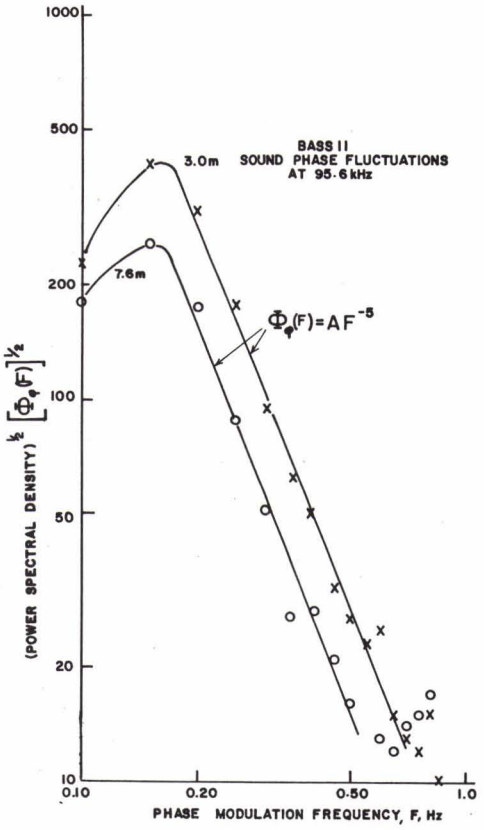

FIG. 4.2
FREQUENCY SPECTRA OF SOUND PHASE FLUCTUATIONS FOR 95.6 kHz SOUND AT DEPTHS 3.0 AND 7.6 m

Acknowledgement

This research was supported by the Office of Naval Research (Code 486.) Mrs. Carol Hickey did the computer calculations of cross sections and damping constants.

REFERENCES

Devin, C., Jr., Survey of thermal, radiation and viscous damping of pulsating air bubbles in water, J. Acoust. Soc. Amer., 31, 1654-1667, (1959).

Eller, A.I., Damping constants of pulsating bubbles. J. Acoust. Soc. Am. 47, 1469-1470,(1970).

Gavrilov, Sov. Phys-Acoust. 15, 22, (1969).

Huffman, T.B. and D.L. Zveare, Sound speed dispersion and inferred microbubbles in the upper ocean. M.S. Thesis, Naval Postgraduate School, Monterey, Ca 93940,(1974).

Medwin et al, Acoustic miniprobing for ocean microstructure and bubbles J. Geophys. Res 80 405-413. (1975).

Medwin, H., In-situ acoustic measurements of bubble populations in coastal ocean waters, J. Geophys. Res., 75, 599-611,(1970).

Medwin, H., Acoustic fluctuations due to microbubbles in the near surface ocean, J. Acoust. Soc. Amer., 56, 1100-1104,(1974).

Phillips, O.M., The Dynamics of the Upper Ocean, p 113, Cambridge University Press, London ,(1966).

Wang, P. C. C., and H. Medwin, Statistical considerations to experiments on the scattering of sound by bubbles in the upper ocean, Quart. J. Appl. Math., 32, 411-425, (1975).